Hindawi
Advances in Condensed Matter Physics
Volume 2019, Article ID 9098256, 9 pages
https://doi.org/10.1155/2019/9098256

Research Article

First Principle Study of the Attachment of Graphene onto Different Terminated Diamond (111) Surfaces

S. Zhao and K. Larsson

Department of Chemistry, Ångström Laboratory, Uppsala University, Uppsala, Sweden

Correspondence should be addressed to K. Larsson; karin.larsson@kemi.uu.se

Received 31 December 2018; Accepted 24 March 2019; Published 2 May 2019

Academic Editor: Ward Beyermann

The adhesion of a graphene monolayer onto terminated or 2x1-reconstructed diamond (111) surfaces has in the present study been theoretically investigated by using a Density Functional Theory (DFT) method. H, F, O, and OH species were used for the surface termination. The generalized gradient spin density approximation (GG(S)A) with the semiempirical dispersion corrections were used in the study of the Van der Waals interactions. There is a weaker interfacial bond (only of type Wan-der-Waals interaction) at a distance around 3 Å (from 2.68 to 3.36 Å) for the interfacial graphene//diamond systems in the present study. The strongest binding of graphene was obtained for the H-terminated surface, with an adhesion energy of -10.6 eV. In contrast, the weakest binding of graphene was obtained for F-termination (with an adhesion energy of -2.9 eV). For all situations in the present study, the graphene layer was found to retain its aromatic character. In spite of this, a certain degree of electron transfer was observed to take place from graphene to O_{ontop}-, O_{bridge}-, and OH-terminated diamond surface. In addition, graphene attached to O_{ontop}-terminated surface showed a finite band gap.

1. Introduction

2D crystalline graphene is unique due to its special band structure. The π and π^* bands of graphene show a linear dispersion around the Fermi level, and they are joined in a single point (i.e., a Dirac point). Graphene possesses high carrier mobility (which can be affected by the surface), saturation velocity, high stability, good electrical and thermal conductivity under ambient conditions, etc. [1–3]. The attractive physical and chemical properties make it popular in many potential applications [4]. However, due to the zero band gap, there is a limitation to use graphene in a transistor device [5]. Thus, it is quite interesting and important to create one sizeable and well-defined band gap without reducing the carrier transport properties of intrinsic graphene. When positioning graphene epitaxially on some surfaces, the perfect graphene 2D structure can become deformed in the third dimension, which thereby affects the electronic properties of graphene.

For the growth of epitaxial graphene onto a $Si/SiC/SiO_2$ substrate, the $Si/SiC/SiO_2$ was observed to limit the carrier mobility by causing additional scattering from charged surface states and impurities, low surface phonon energy, and large trap density. SiO_2 is highly thermally resistive, which will limit the intrinsic properties of graphene and thereby reduce the current capacity of graphene [6, 7]. Diamond has recently been introduced as a good surface for epitaxial graphene. Experimental work has suggested that, by replacing SiO_2 with diamond, it will be possible to achieve a high current-carrying capacitance of intrinsic graphene and to increase the breakdown current density of grapheme [6]. Diamond consists of only sp^3-hybridized carbon atoms. It has a large band gap and possesses excellent properties such as high thermal stability, radiation hardness, chemical resistance, and heat dissipation [7]. There have been some experimental studies on the electronic properties and synthesis of this sp^2 (graphene)-on-sp^3 (diamond) system [6, 8–12]. The graphene-on-diamond system has also been explored in many applications such as high-frequency graphene transistors [13] and spin-polarized conducting wires [14].

The interaction of epitaxial graphene onto diamond surfaces has earlier been theoretically studied [15–17]. The interaction between graphene and clean nondoped (or doped) diamond surfaces has also recently been studied by the present authors. However, the detailed interactions between graphene and different terminated diamond surfaces are still unknown. The unpaired electrons on the surface C atoms are usually passivated by terminations with different atomic or molecular adsorbates. The diamond surface can also passivate these radical C atoms by undertaking surface reconstruction. The 2x1-reconstructed diamond (111) surface has no dangling carbon bonds on the surface. Thus, this saturated surface has been used as a reference surface in this study comparing with different adsorbates passivated diamond (111) surfaces. The most commonly used adsorbates are O, OH, H, and F. The terminating species, which are used with the purpose to uphold the cubic structure of the diamond surface, will not only improve the quality of the diamond surface, but also most often influence the surface electronic structure. The phenomena of diamond surface termination have experimentally been observed to significantly influence the electron affinity, reactivity, and conductivity [18–21]. Therefore, it is quite important to achieve a deeper understanding about the interaction between graphene and the adsorbates on the diamond surface. More specifically, the aim of this study has been to study the energetic stability and electronic properties of graphene attached to diamond (111) surfaces with different termination types (H-, F-, O_{ontop}-, OH-, and O_{bridge}-) compared with reconstructed diamond (111)-2x1 surface. It is a theoretical study based on DFT calculations under periodic boundary conditions. A similar study on nonterminated, but doped, diamond (111) surfaces has earlier been performed by the present authors. B- and N-doped diamond surfaces where then compared with nondoped surface [22]. Because of the small crystallographic lattice mismatch (2%) between graphene and the diamond (111) surface, this specific diamond surface is promising as a substrate for the growth of epitaxial graphene. Hence, this structural similarity between the diamond (111) surface and graphene makes diamond (111) a most suitable surface in studying the effects by diamond surface termination on the interaction between graphene and diamond (111). In order to investigate the effects of different terminations, the adhesion energy of the epitaxial graphene and the electronic structures when adsorbed on different terminated diamond (111) surfaces have here been calculated and analysed.

2. Computational Methods

Geometrical structures of different diamond (111)/graphene interfaces have in the present study been calculated by using Density Functional Theory (DFT) (using the CASTEP software from BIOVIA [23–25]) and so was also total energies and electronic properties of the same systems. These calculations were based on an ultrasoft pseudopotential plane-wave approach under periodic boundary conditions [26]. Moreover, a spin-polarized Perdew Burke Ernzerhof (PBE) functional was used (from here on referred to as a Gradient Generalized Approximation method, GGA), augmented with the Tkatchenko-Scheffler Van Der Waals (TS-VdW) correction [27]. Van der Waals (vdW) interactions is very important to be able to handle in a theoretical study of a diamond/graphene system. The reason is that standard DFT methods cannot properly describe the weak vdW interactions.

Moreover, the plane-wave energy cutoff was set to 380.00 eV, which has earlier been found adequate to use for the present type of study [28]. In addition, the Monkhorst-Pack [29] scheme was used in generating a uniform mesh of k points in the reciprocal space (1×1×1). This mesh has also earlier been found adequate to use for this type of study. [30].

The possibility for electron transfer between the diamond surface and the attached monolayer of graphene has also been calculated by using electron density difference plots and calculated density of states (DOS) spectra. The electron density differences are calculated with respect to the variously terminated diamond surface and to the graphene sheet (see (1)). These density differences give, hence, information about the electron redistribution when attaching a monolayer of graphene onto diamond (111).

$$\Delta\rho = \rho_{diamond/graphene} - \left(\rho_{diamond} + \rho_{graphene}\right) \quad (1)$$

where $\rho_{diamond/graphene}$, $\rho_{diamond}$, and $\rho_{graphene}$ are the electron density of the diamond/graphene system, terminated diamond (111) surface, and graphene monolayer, respectively.

3. Models

A terminated diamond (111) surface, with an epitaxially adhered monolayer of graphene, is used as a supercell model in the present study. The very low lattice mismatch between diamond (111) and graphene (2%) is the reason to the choice of diamond surface plane. The models of systems of graphene and H-terminated and reconstructed 2×1 diamond (111) without any adsorbates are shown in Figure 1.

The diamond/graphene interface model includes diamond 6 C layers (each containing 16 atoms) and 32 C atoms within the graphene sheet. The energetically most stable distance between the diamond (111) surface and graphene was looked for by adjusting (manually) the distance between diamond and graphene, and for each distance calculate the total energy of the diamond/graphene system. Moreover, earlier theoretical studies have shown that 6 C layers are adequate to use in the study of diamond surface properties and structures [31].

H-, OH-, F-, O_{ontop}-, and O_{bridge}-terminated diamond (111) surfaces, as well as a nonterminated reconstructed diamond (111)-2x1 surface, were in the present study used as surfaces for the graphene epitaxial adhesion. The lowest positioned diamond carbon layer atoms were terminated with hydrogen atoms, and both of those layers were kept fixed during the geometry optimization in order to simulate the continuation of bulk diamond. All other atoms were allowed to be completely relaxed in a geometry optimization process using the BFGS algorithm (Broyden–Fletcher–Goldfarb–Shanno) [32]. The vacuum layer within the supercell was, as a result of test calculations, set at a minimum of 15 Å in order to avoid

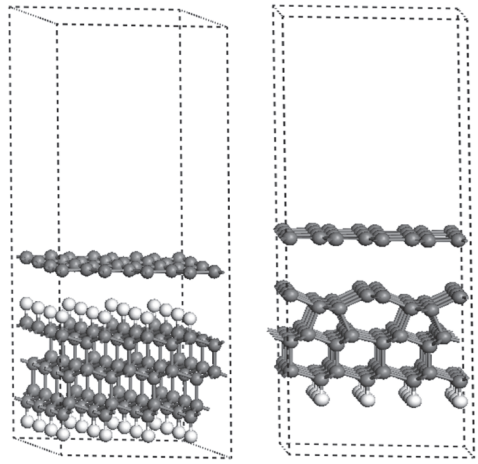

(a) (b)

Figure 1: Side view of graphene on top of a (a) H-terminated diamond (111) surface, and on top of (b) a nonterminated reconstructed diamond (111)-2×1 surface. The H and C atoms are shown in white and gray colour, respectively.

interactions between graphene and the diamond surface in the neighbouring cell.

4. Results and Discussion

4.1. Adhesion Energy and Geometrical Structure of Graphene Adhered onto a Diamond (111) Surface

4.1.1. General. In the search for the optimal graphene// diamond (GD) interfacial distance, the separation between the attached graphene ad-layer and the diamond surface was varied from 2 Å to 5Å, at step sizes of 0.2Å. Geometry optimizations were performed, for each of these diamond-graphene distances, with the purpose of identifying the energetically most preferred interfacial structure. Adhesion energies for the monolayer of graphene attached to the terminated diamond (111) surfaces were thereafter calculated by using

$$E_{adhesion} = \frac{1}{n}\left[E_{diamond-graphene} - E_{diamond} - E_{graphene}\right] \quad (2)$$

where $E_{diamond-graphene}$, $E_{diamond}$, and $E_{graphene}$ are the energies of the whole system, the diamond (111) surface, and the monolayer graphene sheet, respectively. In order to make it possible to compare these results with results for other supercell sizes, these adhesion energies have here been divided with the total number of graphene C atoms in the supercell (n).

4.1.2. Calculations of Geometrical Structures and Adhesion Energies Using the GGA Functional with TS-vdW Corrections. The calculated results of the adhesion energies, in addition to the diamond-graphene interlayer distances, are shown in Table 1. The adhesion energy for all systems is quite small. Hence, the interactions between the diamond surface and the attached monolayer of graphene are all quite weak. Moreover, one can observe that the adhesion energies for all GD systems are negative and thus all adhesion processes are exothermic. The most obvious conclusion from Table 1 is that the shorter the interfacial distance, the more pronounced the adhesion energy (i.e., more negative adhesion energies) (the exceptions from this conclusion are the OH- and O_{bridge}-terminated diamond (111), and the nonterminated 2x1-reconstructed (111) surface). Hence, it is possible to conclude that the larger the interfacial distance, the weaker the interfacial interaction between the ad-layer graphene and the terminated diamond surface. The shortest distance between the graphene monolayer and the H-terminated diamond surface is 2.68 Å, which is correlated with the adhesion energy of -10.6 kJ/mol. The largest graphene adhesion energy is obtained for an F-terminated diamond surface (-2.9 kJ/mol) at an interfacial distance of 3.11 Å. There is, hence, a weaker interaction between graphene and the F-terminated diamond surface, which will be explained more in detail in the following section.

As mentioned above, there are exceptions to this clear correlation between interfacial distance and adhesion energy. For the O-related adsorbates (O_{ontop}, OH, and O_{bridge}), the interfacial distances are quite similar (3.00 Å for O_{ontop}, 2.94 Å for OH, and 2.97 for O_{bridge}). However, the adsorption energies do vary (-7.8 kJ/mol for O_{ontop}, -4.8 kJ/mol for OH, and -5.4 kJ/mol for O_{bridge}). Hence, the interactions between graphene and these diamond surfaces seem to be of different types. As will be shown in Section 4.2, an O_{ontop}-terminated diamond surface shows the strongest interaction with the graphene ad-layer.

Moreover, the interfacial distance for a nonterminated reconstructed 2×1 diamond surface is 3.36 Å whilst the adhesion energy is quite different (-6.69 kJ/mol). This interfacial distance is very close to the interfacial distance (3.35 Å) between different graphene layers in graphite.

Furthermore, it was also observed that the geometry of the terminated diamond surfaces will not change when adding graphene on top of them. This was also the situation

Table 1: Interface distances and adhesion energies for a monolayer of graphene adhered to a nonterminated 2×1-reconstructed diamond (111) surface, or to H-, F-, O_{ontop}-, OH-, and O_{bridge}-terminated diamond (111) surfaces, respectively.

Diamond (111) Surface	Interface Distance (Å)	Adhesion Energy (eV)	Adhesion Energy (eV)
H-Diamond	2.68	-0.11	-10.6
F-Diamond	3.11	-0.03	-2.9
O_{ontop}-Diamond	3.00	-0.08	-7.7
OH-Diamond	2.94	-0.05	-4.8
O_{bridge}-Diamond	2.97	-0.05	-5.4
Reconstructed 2×1-Diamond	3.36	-0.07	-6.7

for the nonterminated diamond surface. When initially positioning a monolayer of graphene quite close to the diamond surfaces (in a range of 1.5 to 2 Å), the graphene layer was found to repel from the terminated diamond surface to an interfacial distance of more than 2.6 Å. As was found in an earlier investigation by the present authors, where nonterminated diamond surfaces were used in the calculations, there is an energy barrier that has to be overcome in order for the graphene sheet to chemisorb to the diamond surface. In the present paper, the dangling surface carbon bonds have been saturated by various species (H, F, O, and OH), or they have been eliminated by reconstructing the surface carbon atoms, and it is thus even harder for the graphene sheet to form covalent bonds with the terminated diamond surface. Thus, the graphene ad-layer prefers to interact with Van der Waals interaction towards the diamond surfaces in the present investigation.

4.2. Electronic Structure for Graphene Adhered onto a Diamond (111) Surface

4.2.1. General. The diamond (111) surface has been 2x1-reconstructed (as a nonterminated surface) or terminated with various species (H, F, OH, and O). The electronegativity differences between the carbon atoms and the adsorbates will result in surface polarization. Moreover, physisorbed epitaxial graphene onto the diamond surface is expected to influence the diamond surface electronic properties. In addition, the terminated diamond surface is expected to affect the electronic properties of graphene. It is thereby interesting to study the electronic interactions between graphene and the diamond surfaces by analysing the electronic structure of various interfacial systems. Electron density differences, band structures, and density of states (DOS) spectra have for this purpose been used as technical tools.

4.2.2. Calculation of Electron Density Differences. An earlier study on nondoped diamond (111) surfaces showed that, for the energetically preferred diamond-graphene distance, there is no covalent bond formation. This is still the situation for graphene on top of a 2x1-reconstructed, or terminated, diamond (111) surfaces. Within the present study, more detailed information about the binding situations within the interfaces of the GD (graphene//diamond) systems has been given as a result of electron density difference calculations. This method is described in Section 2. *Computational Details*. These types of calculations do not only give information about interfacial binding, but also about the occurrence of electron transfer over the interface. Both electron accumulation (red colour) and electron depletion (blue colour) can be seen in Figure 2. These values are calculated with respect to an isolated graphene sheet and an isolated diamond (111) surface.

For all GD systems, there are no electron accumulation between the graphene carbon atoms and the diamond surface atoms within the interfacial space. This observation confirms the lack of covalent bonds between graphene and all terminated or reconstructed diamond (111) surfaces. As can be seen in Figure 2, there are different intensities in colour in the various plots. A more intense colour indicates a more pronounced electronic interaction between graphene and the diamond (111) surface. It is quite apparent that the O_{ontop}-terminated diamond systems showed the most intense colour of electron density difference. Thus, the interaction between the graphene ad-layer and the O_{ontop}-terminated diamond (111) surface is the strongest of the various interfacial systems studied. There is large electron depletion (intense blue colour) at the π orbitals of the graphene C atoms, a small electron accumulation (light red) at the σ orbitals of the graphene C, and a large electron accumulation (dark red) at the site of the O_{ontop} adsorbates. In addition, some electron redistribution takes place inside the graphene ad-layer when attaching graphene on an O_{ontop}-terminated diamond surface. However, there is in total an electron transfer from graphene towards the O_{ontop}–terminated diamond surface. For the other oxygen-related surface terminations (OH- and O_{bridge}-), the situations were found to be almost the same, but with much weaker interfacial interactions. Electron redistribution takes place also within the graphene ad-layer. There is a small electron depletion on several of the graphene carbon atoms that are situated just above the O atom (in OH and O_{bridge}) and some small electron accumulation on the graphene C atoms close to the electron depleted C atoms. Moreover, there are also some small electron accumulations on the O atoms (in OH and O_{bridge}) in both the GOHD (graphene and OH-terminated diamond) and $GO_{bridge}D$ (graphene and O_{bridge}-terminated diamond) systems. Thus, it is possible to state that the O-related adsorbates can induce some electron redistribution within the graphene ad-layer when attaching graphene on top of the terminated diamond surfaces. In addition, there is a minor charge being

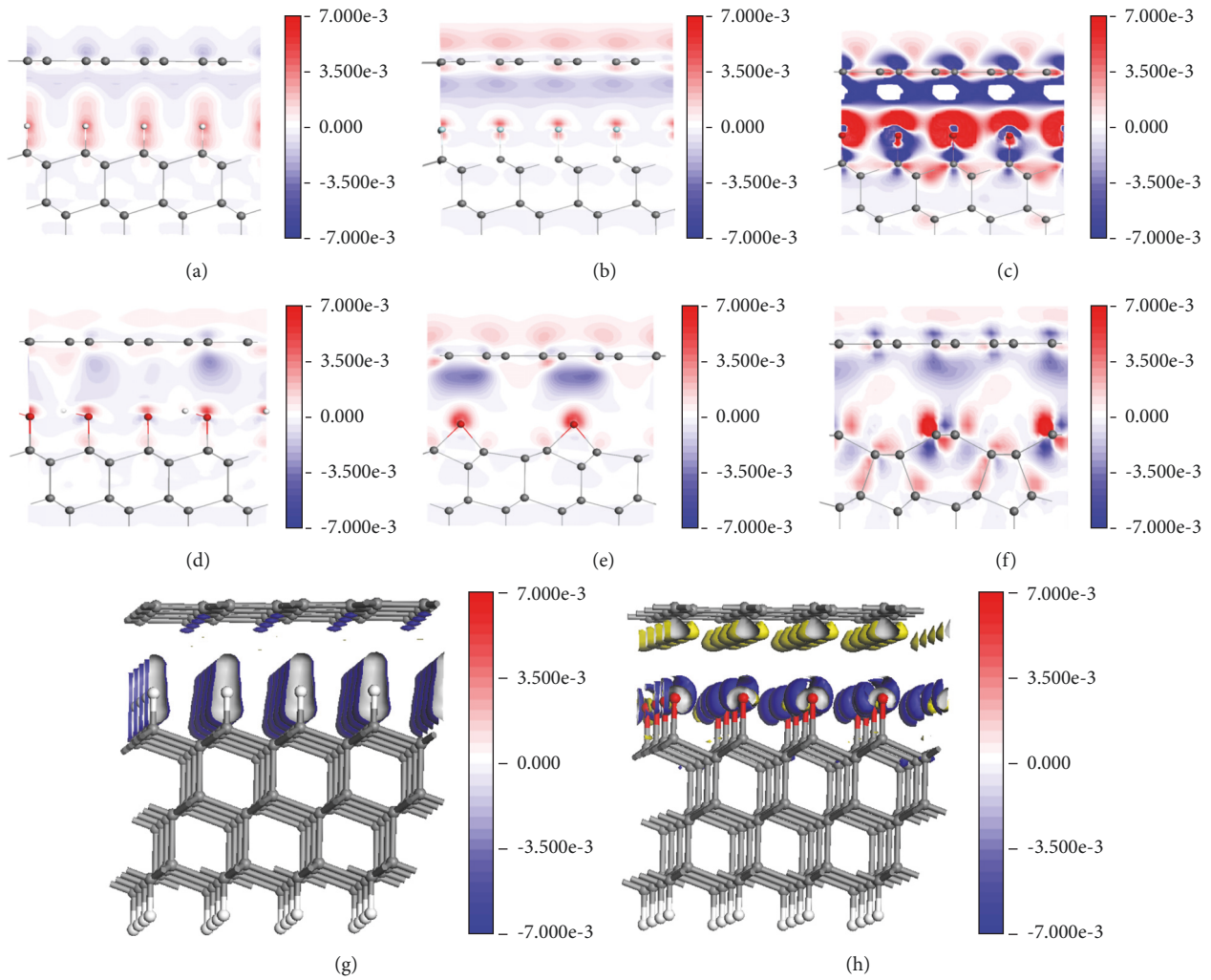

FIGURE 2: Side view of the electron density difference for a (a) GHD system, (b) GFD system, (c) $GO_{ontop}D$ system, (d) GOHD system, (e) $GO_{bridge}D$ system, (f) GD2×1 system, (g) GHD system, and (h) $GO_{ontop}D$ system. The isosurface for (a)-(g) was set to 0.001/Å, and the isosurface for (h) was set to 0.015/Å. The H, O, C, and F atoms are shown in white, red, gray, and green, respectively. The colour scale in the plots goes from $\Delta\rho$=-0.007/Å^3 (blue) to $\Delta\rho$=0.007/Å^3 (red).

transferred between graphene and the OH- and O_{bridge}-terminated diamond (111) surface.

The calculated electron density difference maps were found to be somewhat different for the H- and F-terminated surfaces. In the GFD (graphene and F-terminated diamond) system, there is quite a minor electron accumulation on the F adsorbates and above the C atoms within graphene (with smaller red isosurface). These results confirm that the GFD system is the system that involves the smallest electronic interactions between the diamond surface and the adhered graphene sheet. This agrees well with results from the Section 4.1, where it shows that the F-terminated diamond surface experiences the weakest interaction between graphene and the diamond surface (of all surface terminations studied). The adsorption energy (-2.9 kJ/mol) is thereby the largest one in the present study.

Different from the GFD system, the electrons within the H-terminated diamond are mainly redistributed on the C-H bonds. It should be stressed that the smaller interfacial distance between graphene and the H-terminated diamond surface (2.68 Å) is coupled to stronger atomic interactions (stronger Van der Waals interaction and thus larger adsorption energy) than that for the GFD system (with a larger interfacial distance of 3.11Å). Besides the electron redistribution within the C-H bonds, blue colour (electron accumulation) is present within the interfacial space between graphene and the H-terminated diamond surface. In addition, there is no visible electron density difference within the graphene ad-layer. For comparison, the electron density different plots of GHD and $GO_{ontop}D$ are shown in Figures 2(g) and 2(h). For these two plots, the isosurface values have been chosen differently due to the varied magnitude of interactions between graphene and the terminated diamond surfaces. When decreasing the values of the isosurface, there is no additional appearance of new spheres around the atoms in these systems. For the $GO_{ontop}D$ system, there is large

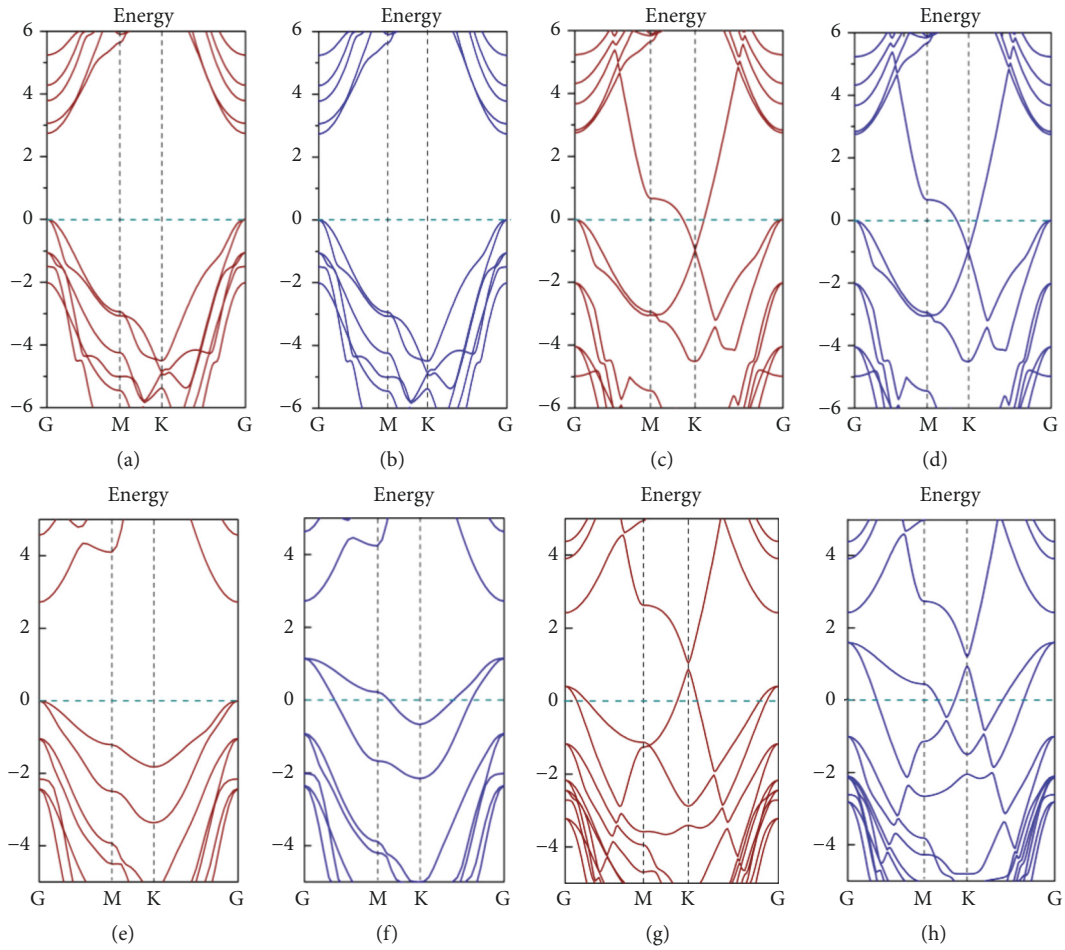

FIGURE 3: The electronic band structure of an (a, b) H-terminated diamond (111) surface, a (c, d) GHD system, an (e, f) O_{ontop}-terminated diamond (111) surface, and a (g, h) $GO_{ontop}D$ system. The (a), (c), (e), and (g) figures represent spin-up states, and the (b),(d), (f), and (h) figures represent spin-down states. The Fermi level is set to zero and is marked by dashed lines at zero energy.

electron depletion on the π orbitals of the graphene C atoms. Thus, there is an electron transfer from graphene towards the O_{ontop}-terminated diamond surface. This agrees with the results shown in Figure 2(c). Moreover, in the GHD system there is a minor electron accumulation on the C atoms just above the H adsorbates on the diamond surface. Hence, it is possible to conclude that there is a minor electron transfer from the H-terminated diamond surface to the adhered graphene ad-layer.

In summary, the here presented electron density different maps do (generally) strongly correlate with the calculated adsorption energies (as presented in Section 4.1). With few exceptions, there is a minor degree of electron transfer between the diamond surface and the attached epitaxial graphene sheet. As an exception, there is quite a small electronic interaction between graphene and the F-terminated diamond surface with almost no electron transfer taken place. The direction of electron transfer for the O_{ontop}- and OH-terminated diamond surface is from graphene to the diamond surface. It is the opposite for the H-terminated diamond surface for which the electron transfer takes place from the diamond surface to the graphene ad-layer. The direction of electron transfer over the diamond-graphene interface will be further presented and discussed in the following section.

4.3. The Band Structure of Graphene//Diamond Systems. It is reasonable to expect that when positioning a graphene layer on top of a diamond surface, the interaction with the surface will induce some band opening. This property can be quite important when using graphene in switching electronic devices. Within the present study, the shapes of the band structures for both the diamond surfaces and graphene (within the GD systems) are quite similar as the ones for intrinsic terminated diamond (111) and graphene, respectively. For all GD systems investigated, there are no mixing states for graphene and the diamond surfaces. This circumstance indicates very weak interactions between the diamond surface and its adhered monolayer of graphene.

As can be seen in Figures 3(c) and 3(d) for the GHD system, the band gap opening of the graphene ad-layer at the Dirac point is quite small. These band gap values of graphene on top of an H-terminated diamond (111) surface are smaller than k_BT (25 meV) at room temperature. This agrees well with the results by Hu et al., who predicted theoretically that

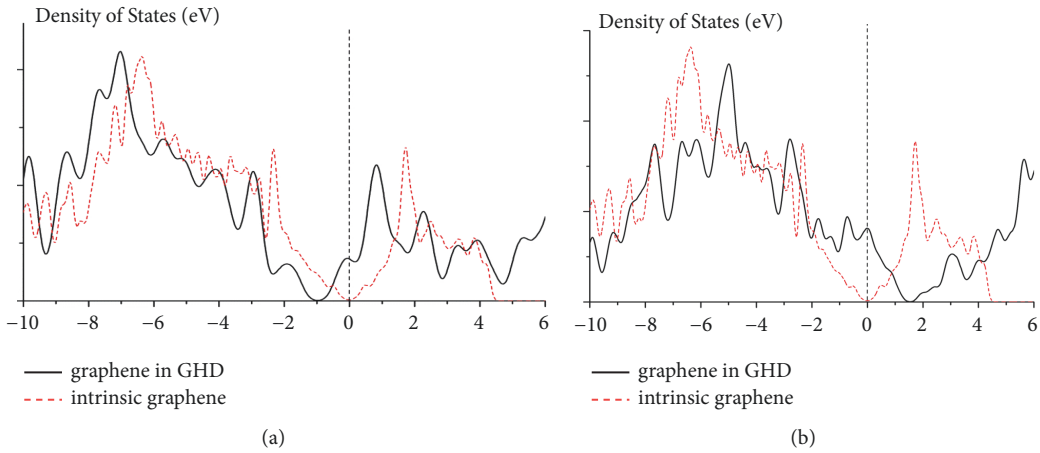

FIGURE 4: Calculated DOS plots for intrinsic graphene (red dashed) in addition to (a) a monolayer graphene adhered to an H-terminated diamond surface (black), or (b) a monolayer graphene adhered to an O_{ontop}-terminated diamond surface (black). The Fermi level is indicated by a black dashed line.

there is no band gap opening for graphene when attached to an H-terminated diamond surface [15]. Within the present study, GFD, $GO_{bridge}D$, and GOHD systems also showed band gaps that where smaller than k_BT (25 meV) at room temperature, which is similar to the GHD system. Hence, the H-, F-, O_{bridge}-, and OH- terminated diamond surfaces will not affect the electronic structure of the graphene ad-layer. However, there are some differences between these band structures. For the GFD, $GO_{bridge}D$, and GOHD systems, the Fermi level crosses the Dirac point, which is identical to the situation for intrinsic graphene. However, for the GHD systems, the Dirac point is -0.97 eV below the Fermi level of the intrinsic graphene (see Figure 4(a)). The main reason for this observation is the negative electron affinity of the H-terminated diamond surface. Moreover, the work function of a monolayer of graphene is even larger than the work function of an H-terminated diamond surface. The VBM (valence band maximum) for the diamond surface lies, hence, above the Dirac point for epitaxial graphene. Thus, an electron transfer from the H-terminated diamond surface to a monolayer of graphene is expected to take place. As was shown in Section 4.2, the results from electron density differences also proved this point. It is, thus, possible to state that a monolayer of graphene, attached to an H-terminated diamond surface, is n-type doped.

Furthermore, because of the comparably strong effect by the O_{ontop} -terminated diamond substrate on the adhesion of epitaxial graphene, a small bandgap at the Dirac point is to be expected. In the $GO_{ontop}D$ system, electrons will thereby be transferred from the graphene monolayer to the O_{ontop}-terminated diamond surface.

In Figure 4(b), a comparison between the density of states for intrinsic graphene and for the O_{ontop}-terminated diamond-supported graphene has been made. The dispersion of states for the two systems is quite similar. However, for the $GO_{ontop}D$ system, the Fermi level of graphene is down-shifted with respect to the Dirac point by almost 1 eV. This is because the work function of an O_{ontop}-terminated diamond surface is larger than the work function for a monolayer of graphene. Thus, the attached monolayer of graphene will be p-type doped. Hence, there will be a hole accumulation within the graphene ad-layer since electrons have been transferred from the monolayer of graphene to the O_{ontop} -terminated diamond surface. This phenomenon of electron transfer was also observed in the calculations of electron density differences and atomic charges.

The band structure of the O_{ontop}-terminated diamond (111) surface is shown in Figures 3(e) and 3(f), and so is also the spin polarized band structure for the $GO_{ontop}D$ system in Figures 3(f) and 3(h). The O_{ontop}-terminated diamond surface has an induced spin polarization within the attached graphene ad-layer. The band structure around the Femi level of the $GO_{ontop}D$ system is quite different from that of the O_{ontop}-terminated diamond. The Dirac point shifts up above the Fermi level, which agrees with results from the DOS calculations (as shown in Figure 4(b)). There is also a noticeable, but small, band gap opening of abound 200 meV at the Dirac point for the graphene ad-layer in the $GO_{ontop}D$ system, which is larger than k_BT (25meV) at room temperature. Hence, the graphene ad-layer will act as a semiconductor with a finite direct small band gap without diminishing other main characteristics of intrinsic graphene (e.g., the zero band gap). These findings improve the possibility of using graphene in a variety of electronic device (i.e., to use the graphene ad-layer in a transistor for switching on/off devices).

5. Summary and Conclusions

In the present study, the DFT method has been used in studying the energetic and electronic interactions between a monolayer graphene and variously terminated diamond (111) surfaces or nonterminated 2x1 reconstructed diamond (111) surfaces. It has been concluded that there is only Van der Waals interactions between the graphene ad-layer and the H-, OH-, F-, O_{ontop}-, or O_{bridge}-terminated, or the nonterminated

2x1-reconstructed, diamond (111) surface. It has been shown that the adsorbates can affect the adsorption energy of an attached graphene sheet on top of terminated diamond surfaces. The H adsorbates on the diamond (111) surface were found to provide the largest interaction with the graphene ad-layer (with an adsorption energy of -10.6 eV). In contrast, the smallest diamond-graphene interaction was observed for F-termination of the diamond surface (with an adsorption energy of -2.9 eV). In addition, a partial electron transfer was observed to take place between the graphene ad-layer and the H-, O_{ontop}-, OH-, or O_{bridge}-terminated diamond surface. There is in total an electron transfer from graphene towards the O_{ontop}-, OH-, and O_{bridge}-terminated diamond surface. On the contrary, there is an electron transfer from the H-terminated diamond surface towards the graphene ad-layer. Moreover, the O_{ontop-}terminated surface was found to have the strongest interaction with the epitaxial monolayer of graphene. The system of graphene and O_{ontop-}terminated diamond shows the largest electron transfer. Moreover, a monolayer of graphene, attached to an O_{ontop-}terminated diamond surface, showed a finite band gap. This observation is very promising for the use of diamond-supported graphene in transistor devices.

Data Availability

The theoretical data used to support the findings of this study are included within the article.

Conflicts of Interest

The authors declare that they have no conflicts of interest.

Acknowledgments

This work was supported by the Swedish Research Council (VR). The results were generated using CASTEP, Material Studio which is developed by BIOVIA Inc. The results in this work are included in the thesis by one of the authors (Shuainan Zhao), *Digital Comprehensive Summaries of Uppsala Dissertations from the Faculty of Science and Technology 1370*.

References

[1] A. H. Castro Neto, F. Guinea, N. M. R. Peres, K. S. Novoselov, and A. K. Geim, "The electronic properties of graphene," *Reviews of Modern Physics*, vol. 81, no. 1, pp. 109–162, 2009.

[2] K. I. Bolotin, K. J. Sikes, Z. Jiang et al., "Ultrahigh electron mobility in suspended graphene," *Solid State Communications*, vol. 146, no. 9-10, pp. 351–355, 2008.

[3] A. A. Balandin, S. Ghosh, W. Bao et al., "Superior thermal conductivity of single-layer graphene," *Nano Letters*, vol. 8, pp. 902–907, 2008.

[4] A. K. Geim and K. S. Novoselov, "The rise of graphene," *Nature Materials*, vol. 6, no. 3, pp. 183–191, 2007.

[5] F. Schwierz, "Graphene transistors," *Nature Nanotechnology*, vol. 5, no. 7, pp. 487–496, 2010.

[6] J. Yu, G. Liu, A. V. Sumant, V. Goyal, and A. A. Balandin, "Graphene-on-diamond devices with increased current-carrying capacity: Carbon sp 2-on-sp 3 technology," *Nano Letters*, vol. 12, no. 3, pp. 1603–1608, 2012.

[7] A. Kraft, "Doped diamond: A compact review on a new, versatile electrode material," *International Journal of Electrochemical Science*, vol. 2, no. 5, pp. 355–385, 2007.

[8] F. Zhao, A. Afandi, and R. B. Jackman, "Graphene diamond-like carbon films heterostructure," *Applied Physics Letters*, vol. 106, no. 10, 2015.

[9] S. P. Cooil, F. Song, G. T. Williams et al., "Iron-mediated growth of epitaxial graphene on SiC and diamond," *Carbon*, vol. 50, no. 14, pp. 5099–5105, 2012.

[10] F. Zhao, T. Thuong Nguyen, M. Golsharifi, S. Amakubo, K. P. Loh, and R. B. Jackman, "Electronic properties of graphene-single crystal diamond heterostructures," *Journal of Applied Physics*, vol. 114, no. 5, Article ID 053709, 2013.

[11] D. Varshney, C. Venkateswara Rao, M. J. Guinel, Y. Ishikawa, B. R. Weiner, and G. Morell, "Free standing graphene-diamond hybrid films and their electron emission properties," *Journal of Applied Physics*, vol. 110, no. 4, Article ID 044324, 2011.

[12] F. Zhao, T. T. Nguyen, and M. Golsharifi, "Electronic properties of graphene-single crystal diamond heterostructures," *Journal of Applied Physics*, vol. 114, Article ID 053709, 2013.

[13] Y. Wu, Y.-M. Lin, A. A. Bol et al., "High-frequency, scaled graphene transistors on diamond-like carbon," *Nature*, vol. 472, no. 7341, pp. 74–78, 2011.

[14] T. Shiga, S. Konabe, J. Shiomi, T. Yamamoto, S. Maruyama, and S. Okada, "Graphene-diamond hybrid structure as spin-polarized conducting wire with thermally efficient heat sinks," *Applied Physics Letters*, vol. 100, no. 23, 2012.

[15] Y. Ma, Y. Dai, M. Guo, and B. Huang, "Graphene-diamond interface: Gap opening and electronic spin injection," *Physical Review B: Condensed Matter and Materials Physics*, vol. 85, no. 23, 2012.

[16] W. Hu, Z. Li, and J. Yang, "Diamond as an inert substrate of graphene," *The Journal of Chemical Physics*, vol. 138, no. 5, Article ID 054701, 2013.

[17] D. Selli, I. Baburin, S. Leoni, Z. Zhu, D. Tománek, and G. Seifert, "Theoretical investigation of the electronic structure and quantum transport in the graphene–C(111) diamond surface system," *Journal of Physics: Condensed Matter*, vol. 25, no. 43, Article ID 435302, 2013.

[18] B. L. Mackey, J. N. Russell Jr., J. E. Crowell, and J. E. Butler, "Effect of surface termination on the electrical conductivity and broad-band internal infrared reflectance of a diamond (110) surface," *Physical Review B: Condensed Matter and Materials Physics*, vol. 52, no. 24, pp. R17009–R17012, 1995.

[19] J. A. Garrido, A. Härtl, M. Dankerl et al., "The surface conductivity at the diamond/aqueous electrolyte interface," *Journal of the American Chemical Society*, vol. 130, no. 12, pp. 4177–4181, 2008.

[20] F. K. De Theije, O. Roy, N. J. Van Der Laag, and W. J. P. Van Enckevort, "Oxidative etching of diamond," *Diamond and Related Materials*, vol. 9, no. 3, pp. 929–934, 2000.

[21] S. Ferro and A. De Battisti, "The 5-V Window of Polarizability of Fluorinated Diamond Electrodes in Aqueous Solutions," *Analytical Chemistry*, vol. 75, no. 24, pp. 7040–7042, 2003.

[22] S. Zhao and K. Larsson, "First principle study of the attachment of graphene onto non-doped and doped diamond (111)," *Diamond and Related Materials*, vol. 66, pp. 52–60, 2016.

[23] S. J. Clark, M. D. Segall, C. J. Pickard et al., "First principles methods using CASTEP," *Zeitschrift für Kristallographie*, vol. 220, no. 5-6, pp. 567–571, 2005.

[24] P. Hohenberg and W. Kohn, "Inhomogeneous electron gas," *Physical Review*, vol. 136, no. 3B, pp. B864–B871, 1964.

[25] W. Kohn and L. J. Sham, "Self-consistent equations including exchange and correlation effects," *Physical Review A: Atomic, Molecular and Optical Physics*, vol. 140, pp. A1133–A1138, 1965.

[26] D. Vanderbilt, "Soft self-consistent pseudopotentials in a generalized eigenvalue formalism," *Physical Review B: Condensed Matter and Materials Physics*, vol. 41, no. 11, pp. 7892–7895, 1990.

[27] J. P. Perdew, K. Burke, and M. Ernzerhof, "Generalized gradient approximation made simple," *Physical Review Letters*, vol. 77, no. 18, pp. 3865–3868, 1996.

[28] A. Pallas and K. Larsson, "Structure determination of the 4d metal diborides: A quantum mechanical study," *The Journal of Physical Chemistry B*, vol. 110, no. 11, pp. 5367–5371, 2006.

[29] H. J. Monkhorst and J. D. Pack, "Special points for Brillouin-zone integrations," *Physical Review B: Condensed Matter and Materials Physics*, vol. 13, no. 12, pp. 5188–5192, 1976.

[30] S. Zhao and K. Larsson, "Theoretical study of the energetic stability and geometry of terminated and B-doped diamond (111) surfaces," *The Journal of Physical Chemistry C*, vol. 118, no. 4, pp. 1944–1957, 2014.

[31] D. Petrini and K. Larsson, "Origin of the reactivity on the nonterminated (100), (110), and (111) diamond surfaces: An electronic structure DFT study," *The Journal of Physical Chemistry C*, vol. 112, no. 37, pp. 14367–14376, 2008.

[32] T. H. Fischer and J. Almlöf, "General methods for geometry and wave function optimization," *The Journal of Physical Chemistry C*, vol. 96, no. 24, pp. 9768–9774, 1992.